

Equilibrium structure and Ti-catalyzed H₂ desorption in NaAlH₄ nanoparticles from density functional theory

Tejs Vegge*

Received 10th April 2006, Accepted 18th September 2006

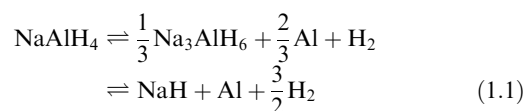
First published as an Advance Article on the web 9th October 2006

DOI: 10.1039/b605079d

Improving the hydrogen ab- and desorption kinetics in complex hydrides is essential if these materials are to be used as reversible hydrogen storage media in the transport sector. Although reductions in particle size and the addition of titanium based compounds have been found to improve the kinetics significantly, the physical understanding remains elusive. Density functional theory is used to calculate the energy of the potential low energy surfaces of NaAlH₄ to establish the equilibrium particle shape, and furthermore to determine the deposition energy of Ti/TiH₂ and the substitutional energy for Ti@Al and Ti@Na-sites on the exposed facets. The substitutional processes are energetically preferred and the Na-vacancy formation energy is found to be strongly reduced in the presence of Ti. The barrier for H₂ desorption is found to depend significantly on surface morphology and in particular on the presence of Ti, where the activation energy for H₂ desorption on NaAlH₄{001} surfaces can drop to 0.98 eV—in good agreement with the experimentally observed activation energy for dehydrogenation.

1. Introduction

The 1997 discovery by Bogdanović and Schwikardi¹ that titanium based additives could catalyze the ab- and desorption of hydrogen in the complex hydride NaAlH₄ sparked new hope that reversible solid state storage of hydrogen was feasible in the transport sector.² A substantial number of research projects focusing on complex hydrides, in particular metal aluminum hydrides (alanates), have subsequently been initiated. In the decomposition of, *e.g.*, NaAlH₄:



the last step is generally not considered reversible for practical applications due to the stability of NaH.

The addition of titanium rich compounds is known to improve the kinetics of the first and second step in both ab- and desorption of hydrogen. At present, two competing theories have been proposed to explain this effect: (i) either titanium forms a catalytically active complex at the surface (with Ti_xAl_y-type species being the favourite³), which assists in the dissociation/recombination of hydrogen^{4–6} and/or structural decomposition; or (ii) the titanium atoms perform bulk substitution with either Al or Na atoms and thereby lower the barrier for diffusion, potentially by simultaneous creation of an unspecified number of vacancies and/or hydrogen interstitials.^{7–9}

The influence of particle size and shape is particularly pronounced at the nanoscale, and it is generally accepted that nano-sized particles display superior kinetics in almost all metal hydride systems. Recent experimental^{10,11} and theoretic^{12–14}

studies, which appear to favor hypothesis (i), have prompted this investigation of surface properties of un/Ti-doped NaAlH₄ nanoparticles with special emphasis on catalytic sites and hydrogen desorption processes. In a systematic approach using density functional theory (DFT) calculations, the surface energy of all potential low energy structures is calculated. Based on these results, a Wulff construction¹⁵ is used to determine the equilibrium particle shape. The binding energy of Ti and TiH₂ as well as the energy of Ti@Al- and Ti@Na-site substitutions in the surface layer are calculated on all exposed facets, where *e.g.* the Na-vacancy formation energy is strongly reduced in the presence of Ti. Combining these observations with the strong thermodynamic driving force for NaCl formation, a viable reaction pathway following TiCl₃ addition emerges, which could potentially lead to the observed superior initial hydrogen desorption kinetics. Furthermore, the barrier for H₂ desorption is found to depend substantially on surface morphology and the presence of Ti. The titanium atoms are found to destabilize the neighboring (AlH₄)^{–1}-complexes by charge depletion and in some cases induce Al–H bond breaking and hydrogen transfer from Al to Ti. This results in a substantial lowering of the activation energies for H₂ desorption as well as final state energies.

2. Computational parameters

The electronic structure calculations in this paper are performed within density functional theory (DFT) using the DACAPO pseudopotential implementation.^{16,17} A plane wave expansion of the Kohn–Sham wavefunctions is performed up to a kinetic energy cutoff-value of 25 Ry and 45 Ry was used as a cutoff for the density grid. Ultra-soft pseudopotentials¹⁸ are used to describe the ionic cores, and the exchange and correlation effects are described using the RPBE functional.¹⁹ The wave functions were sampled according to a

Materials Research Department, Risø National Laboratory, DK-4000 Roskilde, Denmark. E-mail: tejs.vegge@risoe.dk

Monkhorst–Pack scheme²⁰ with a k -points mesh of spacing $\leq 0.1 \text{ \AA}^{-1}$ for all phases. Three-dimensional periodic boundary conditions are applied in the calculations and the surfaces are created by introduction of a vacuum layer. The self-consistent electron density is determined by iterative diagonalization of the Kohn–Sham Hamiltonian, and the resulting Kohn–Sham eigenstates are populated following a Fermi distribution ($k_{\text{B}}T = 0.2 \text{ eV}$); Pulay mixing²¹ of the resulting electronic density is subsequently performed, and finally, all total energies are extrapolated to zero temperature.

2.1. Super-cell setup

The super cells contain up to 195 atoms, where the specifics of the setup in a given calculation depends on the properties of the facet in question, *e.g.* the $\text{NaAlH}_4\{001\}$ surface simulation contains 96 atoms ordered in a (2×2) surface unit cell with a slab thickness of 11.39 \AA ; in addition a 11.4 \AA vacuum layer is placed between the slabs to ensure separation. Equilibrium lattice constants for the tetragonal $I4_1/a$ ground state of NaAlH_4 of $a = 5.031 \text{ \AA}$ and $c = 11.388 \text{ \AA}$ were determined from an energy minimization of a 96 atoms bulk calculation, by performing iterative relaxations of the internal degrees of freedom and the unit cell parameters. The surface super cells are optimized by allowing all the atoms to relax their atomic coordinates, while keeping the surface unit cell fixed.

2.2. Nudged elastic band

The nudged elastic band (NEB) method is used to determine the energy barriers for the activated processes on the potential energy surface.²² The method locates the transition state (TS) between relaxed initial, *e.g.* a relaxed NaAlH_4 surface, and final (a H_2 molecule far above the NaAlH_4 surface) states. The transition path is represented computationally by a sequence of 7 configurations (images), going from the initial (IS) to the final state (FS), which are connected by spring forces in order to ensure continuity along the path; here, a linear interpolation in all atomic coordinates is used as an initial guess. The path is subsequently relaxed to a minimum energy path (MEP), where the forces perpendicular to the path vanish. The saddle point or transition state configuration (TS), *i.e.* the configuration with maximal energy along the MEP, is located *via* the Climbing Image implementation of the NEB method.²³

2.3. Wannier functions

The charge of titanium in the form of individual atoms, small clusters or Ti_xAl_y type complexes is essential for the catalytic properties, and is expected to depend strongly on the local atomic environment. Furthermore, the chemical state of Ti is one of the parameters which can be determined experimentally.²⁴

The electronic ground state of a solid state system can be represented in terms of localized orbitals as described by Wannier,²⁵ and the calculated plane-wave eigenstates can be transformed into a set of localized Wannier functions (WFs). The WFs then provide important chemical information, such as bond types and valence,^{26,27} and the Ti-valence can be used for comparison with experimental EXAFS^{24,28} data to provide information about the chemical state and local atomic configuration around the Ti-atom.

3. Surface energies and equilibrium particle shape

Sodium alanate has a tetragonal ground state structure belonging to the $I4_1/a$ space group (#88). The sodium atoms occupy the $4(a)$ Wyckoff positions, aluminum $4(b)$, and hydrogen the $16(f)$ sites with $x = 0.235$, $y = 0.386$ and $z = 0.547$, and a corresponding calculated bulk reference energy ($Z = 4$) of $E_{\text{bulk}} = -2209.49 \text{ eV}$.

3.1. The energy of low index NaAlH_4 surfaces

Simulations have been performed on the low index surfaces of NaAlH_4 in order to establish the relevant surface energies γ (see Table 1) to determine the equilibrium particle shape. The surfaces are allowed to relax and reorder within the super cell, whereas any potential long range surface reconstructions are not considered (no recorded observations in alanates) since the shear length scale of such reconstructions in ionic insulators²⁹ would render them irrelevant for nanoscale particles.

The $\{112\}$ surfaces have also been included, since the symmetry positions in the tetragonal unit cell provides close packing of the metal atoms in these planes; higher index structures such as $\{114\}$ are even more open and have not been included, since the structures are significantly less dense and unlikely to yield lower energies. A standard definition of the surface energy

$$\gamma = \frac{1}{2}(E_{\text{slab}} - NE_{\text{bulk}}) \quad (3.2)$$

is used, although several different definitions have been applied to account for convergence with slab thickness.^{30,31} For the thick slabs investigated here, the surface energies are found to be fully converged, as described in the following.

The $\{001\}$ facets are the closed packed surfaces and the calculational cell consists of a square surface unit cell with side lengths of 10.06 \AA , totaling a surface area of 202.4 \AA^2 . The slab has a thickness of 11.39 \AA and the surfaces are cleaved to optimize the density while retaining the AlH_4 -complexes, as seen in Fig. 1. The super cell contains 96 atoms, and the surface energy is found to be as low as $\gamma_{001} = 62 \text{ mJ m}^{-2}$, see Table 1.

The (100) and (010) facets of the $\{100\}$ class have been simulated using a rectangular surface unit cell of 10.06 \AA by 11.39 \AA . The slab has a thickness of 10.06 \AA and the unit cell contains 96 atoms. Test calculations on a twice as thick 192 atom slab resulted in the same surface energy. A small difference in energy of $\sim 90 \text{ meV}$ was observed between the (100) and (010) surfaces, although these surface energies should—in principle—be equal due to symmetry. The variation is ascribed to slightly modified H–H distances and the

Table 1 The energy of low index NaAlH_4 surfaces

Surface	E_{sim}/eV	Area/ \AA^2	$\gamma/\text{mJ m}^{-2}$
$\{001\}$	−2208.71	202.4	62
$\{100\}$	−2206.22	229.2	219
$\{110\}^a$	−4416.07	324.1	149
$\{101\}$	−2207.31	250.5	139
$\{112\}^a$	−4416.46	382.1	106

^a The unit cell contains 192 atoms to allow for relaxations of the open surface.

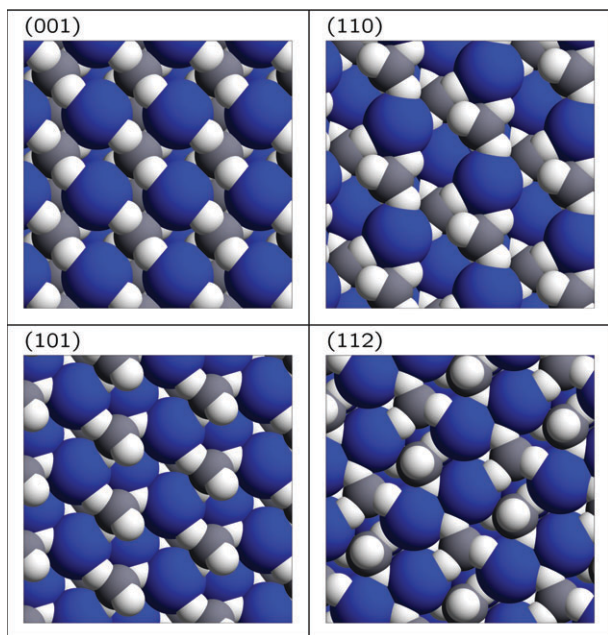


Fig. 1 The figure displays the atomic configuration in the low energy {001}, {110}, {101} and {112} facets, respectively. Sodium atoms are depicted as blue, aluminum atoms as gray, and hydrogen atoms as white.

{100} energy is therefore expected to be representative of all {100} facets (see Table 1); however, with a surface energy $\sim 220 \text{ mJ m}^{-2}$ both facets are found to be energetically unfavored.

The super cell used in the simulation of the {101} surfaces has a rectangular surface unit cell with side lengths of 12.45 and 10.06 Å totaling a surface area of 250.5 Å². The slab is 18.37 Å thick and the super cell contains 96 atoms. The surface is cleaved to obtain an even distribution of Na atoms and AlH₄-complexes (see Fig. 1). The cost of Al–H bond breaking is simply too high, and the applied surface termination was recently shown to have the lowest surface energy for the (101) surface.³⁰ Here, a surface energy of 139 mJ m⁻² is obtained, which is substantially lower than for the {100} facets. Calculations on a slab with twice the thickness and side lengths of 12.45 and 5.03 Å, respectively, verified the slab convergence by yielding the same surface energy.

Due to the open nature of the initial rectangular {110} surface unit cell, a larger unit cell with side lengths of 14.23 and 11.39 Å is used to account for surface relaxations (324.1 Å²). In calculations having only half the slab thickness, the surfaces of the slab were not sufficiently separated and the resulting surface energy was underestimated by 16%. The slab is 14.23 Å thick and the super cell contains 192 atoms, having a surface energy of 149 mJ m⁻². This surface has not previously been investigated, and the surface energy is surprisingly low compared to, *e.g.*, the closer packed {100} facets—the importance of which will be discussed in the following section.

The parallelepiped super cell used to simulate the {112} surfaces has a rhombohedral surface unit cell with a side length of 15.20 Å and a total surface of 382.1 Å², it is 12.05 Å thick and contains 192 atoms. Due to the tetragonal structure and the position of the metal atoms, the {112}

surfaces are closely packed. The simulational setup enforces an upper (112) and a lower ($\bar{1}\bar{1}2$) facet, which are symmetrically inequivalent in $I4_1/a$; the obtained surface energy of 106 mJ m⁻² is therefore an averaged value for the two facets.

In Table 1, the {001} facet is seen to have a very low surface energy, $\gamma_{001} = 62 \text{ mJ m}^{-2}$, whereas the {100} energies are 3–4 times higher than for {001} and substantially higher than for the investigated higher index surface.

4. Equilibrium particle shape

The ab- and desorption kinetics of hydrogen in complex and conventional metal hydrides is generally improved by a reduction of the average grain size to the nanometer range.^{32,33} In order to systematically improve the kinetics by optimizing particle size and/or applied catalysts, it is essential to possess detailed structural information at the atomic scale. Although conventional production techniques do not allow for nanoscale control, atomic level information about binding sites and activity of catalyst on different facets can lead to the selection of superior additives. Such information is accessible, *e.g.*, from the calculated energies of the different surface facets by applying a Wulff construction,¹⁵ which models the equilibrium particle shape by minimizing the area of a given facet according to the relative surface energies, see Fig. 2.

It is interesting to note that the relatively high surface energy of the {100} facets results in preferential cleavage along the substantially more open {110} facets, *i.e.* the {100} facets are not exposed on equilibrium particles. The {112} and {101} surfaces are also exposed, {112} on the edges and {101} at the corners, as shown in Fig. 2.

The multi-faceted shape of the particles significantly increases the number of potential binding sites for catalytic particles/complexes, and hence also the number of potential pathways for hydrogen desorption. In the following, the energetics of potential binding sites for titanium atoms is investigated as well as metal atom substitution of Ti in the surface layer of the exposed facets. In section 6, the barrier for hydrogen desorption is investigated with specific attention to the potential catalytic effect of titanium doping.

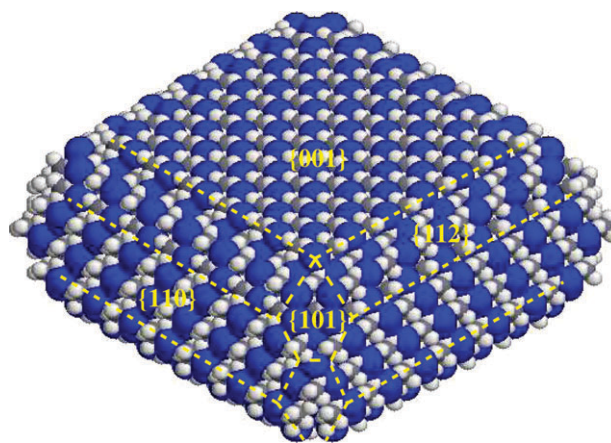


Fig. 2 The equilibrium particle shape according to the Wulff construction. The low surface energy of the {001} type facets is seen to dominate, but {112}, {101} and {110} type facets are also exposed.

5. Titanium deposition and metal atom substitution

Addition of titanium halides or nano-sized $\text{Ti}_{13} \cdot 6\text{THF}$ clusters³⁴ is known to improve the hydrogen desorption kinetics the most, but the physical explanation has remained elusive. A number of different explanations have been proposed for this effect, including a possible catalytic effect of Ti_xAl_y type alloys, which have been shown by several groups to form slowly over a number of sorption cycles,³⁵ but other species like TiH_2 have also been proposed.³⁶ Using either of these compounds directly as a dopant does, however, yield significantly inferior kinetics than using TiCl_3 ,^{37,38} and additional/other effects must therefore be expected.

The possibility of a combined or multiple effect of Ti-based additives, has recently begun to surface in the literature *e.g.* by Brinks *et al.*³⁵ In a recent hydrogen isotope-scrambling experiment Bellosta von Colbe *et al.* also found clear evidence of a multiple effect of titanium doping in uncycled non ball-milled NaAlH_4 samples, but the hydrogen–deuterium exchange rate did not appear to be rate-limiting.⁵ Using electron paramagnetic resonance on NaAlH_4 doped with titanium halides, Craig M. Jensen's group found the profoundly enhanced hydrogen kinetics is due to a titanium species which is present only in a relatively minor amount.³⁹ Similar observations are frequently seen in heterogeneous catalysis where, *e.g.*, a small number of step sites compared to the majority of terrace sites are rate-controlling.^{40,41}

Calculations including $\text{Ti}_{13} \cdot 6\text{THF}$ clusters and their organic linkers are computationally too demanding, so here the effects of atomic titanium and TiCl_3 are investigated on the exposed nanoparticle facets in conjunction with possible metal atom substitution processes in order to locate the preferred titanium sites. Due to the complexity of the mechanisms involved, it is therefore possible that other effects might also contribute to the hydrogen desorption kinetics.

5.1. Ti and TiH_2 binding sites and energies

The local atomic ordering at the preferred bonding sites is found to depend strongly on the characteristics of the surface, and it is observed that the titanium atoms tend to contract into the surface to compensate for their apparent under-coordination, in agreement with the findings of Løvrik on $\text{NaAlH}_4(001)$.¹²

The preferred binding sites of Ti on the respective facets can be seen in Fig. 3, where Ti-atoms are confined to the top-most layer on the closest packed (001) and (112) surfaces, whereas the open (110) surfaces can accommodate the Ti atoms by allowing easy penetration into the surface layer. To analyze changes in the titanium deposition energy, bulk titanium is used as the reference energy. This energy “cost” is in some cases either neglected in theoretical work⁸ or atomic titanium used as a reference.⁴²

There is strong experimental evidence for the formation of the thermodynamically stable Ti_xAl_y type species, but only after a number of sorption cycles. During the initial titanium deposition their formation is kinetically hindered under operational conditions,⁴³ but given the instantaneous effect following doping with titanium halides, another active species is therefore likely to be present.

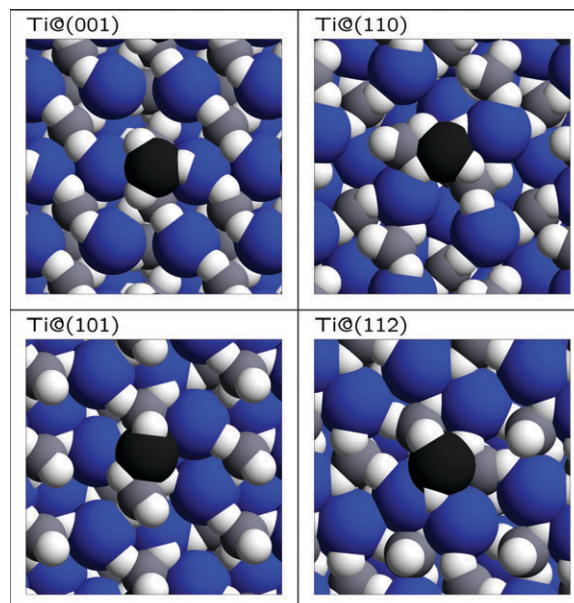


Fig. 3 Titanium binding sites on the (001), (110), (101), and (112) facets. From the figure, it is clear that the Ti (black) contracts into the surface, when possible, and attracts hydrogen atoms from neighboring AlH_4 -complexes. For the relative energies, see Table 2.

The deposition energy of Ti is found to be reduced from 3.4 to 2.0 eV going from the close packed {001} type to the more open {110} surfaces (see Table 2). The effect is primarily attributed to the increased coordination resulting from the surface penetration (see section 7 for further details), and a lower cost would be expected for Ti nano-clusters.

On the (001) surface (see Fig. 3), the titanium atom effectively breaks an Al–H bond and pulls away a hydrogen atom from a neighboring AlH_4 -complex. This illustrates a possible catalytic role of Ti, *i.e.* lowering the formation energy of AlH_3 -type species and the barrier for H_2 desorption. The AlH_3 species could potentially also desorb directly, but this is beyond the scope of this paper and is currently under investigation.⁴⁴

On the more open (110) surface, the Ti-atom is able to coordinate to six nearest neighbor hydrogen atoms at distances of 1.88–2.00 Å and three Al atoms at 2.46–2.94 Å (average of 2.70 Å), without breaking Al–H bonds.

The addition of two hydrogen atoms to the surface titanium was also performed to investigate the effect of changing the Ti-valence. In recent theoretical investigations of bulk substituted Ti in NaAlH_4 , this was found to have a significant effect on hydrogen diffusion.⁴² On all surfaces—except for (110)—the addition of two extra hydrogen atoms to Ti is found to lower the deposition energy. From Table 2 it is seen that the deposition energy on the {001} and {101} surfaces is reduced significantly, whereas the {110} and {112} surfaces remain virtually unchanged. For all surfaces, the cost is still high with respect to bulk Ti; a result which agrees well with the very limited experimental indications of TiH_2 features⁴⁵ when TiCl_3 is used as dopant.

This would require doping directly with TiH_2 or metallic Ti nano-clusters since the unstable atomic titanium is unlikely to remain on the surface long enough to form TiH_2 species. The

Table 2 The energy cost of Ti and TiH₂ deposition and Ti substitution at Al and Na-sites, respectively. All energies are in eV using the ground state of the metals and the H₂ molecule as reference energies

	{001}	{110}	{101}	{112}
Ti	3.4	2.0	3.2	2.9
TiH ₂	2.1	2.1	1.1	2.8
Ti@Al	1.4	1.1	1.6	1.8
Ti@Na	1.9	2.0	1.9	1.7

correct reference energies are thus the NaAlH₄ surface and TiH₂(s), which has a formation energy of 1.18 eV, bringing the true cost to 2.3–4.0 eV. Atomic Ti/TiH₂ appears as a thermodynamically improbable catalytic configuration, in line with Wang *et al.*,³⁸ who observe significantly inferior hydrogen kinetics compared to titanium halides, when metallic Ti or TiH₂ are used directly as dopants.

5.2. Surface substitution processes

Metal atom substitution has been suggested as a potential process for Ti-incorporation at bulk and surface sites,¹² where it can potentially substitute both Al and Na atoms. The preferred configuration could depend on both the chemical state of Ti and the local atomic configuration at the doping site.

Substitution of Ti for Al has recently been shown theoretically to be the preferred substitution in bulk NaAlH₄^{12–14} and recent experimental work by Fichtner *et al.* indicates a weak preference for Al- over Na-sites.⁴⁶ On the NaAlH₄(001) surface, recent theoretical work by Yildirim and Íñiguez⁴⁷ shows the Na-sites to be preferred, whereas Løvnik and Opalka find Ti@Al to be favoured.^{12,13} The difference is primarily due to a difference in the choice of reference energy, where the findings of Løvnik and Opalka are consistent with the work presented here.

Initially, the Ti@Al substitution is investigated in the surface layer on all four exposed facets. The Al⁺³ valence in the (AlH₄)⁻¹-complexes is well matched by titanium, and only a minor restructuring is observed in the TiH₄-type complex on all exposed facets. The neighboring AlH₄-complexes do, however, rotate and the hydrogen atoms are drawn in towards Ti, thus increasing the coordination of the Ti atom (see section 7 for a detailed charge analysis). The substitutional energy cost is seen to depend moderately on the surface coordination (see Table 2), although displaying a clear preference for the {110} surface. The open surface structure on this facet enables easy penetration and reorientation of the neighboring AlH₄-complexes. This observation agrees with Løvnik and Opalka who find Ti@Al substitution to be preferred directly below the surface on the more compact {001} surface.¹² However, an energy cost of 1.1 eV renders this substitution unlikely unless other simultaneous processes are involved in the initial deposition reaction.

For Ti@Na substitution, it is apparent from Table 2 that the energy cost is even higher than for the Al-sites, as observed by Løvnik and Opalka,^{12,13} and also less dependent on the corrugation of the surface. With a cost in excess of 1.7 eV, this process appears unlikely, unless other initial effects, such as partial decomposition or the strong thermodynamic driving force for NaCl formation are considered. In the case of doping

with TiCl₃—a premier catalytic additive—the NaCl formation is highly relevant.

Compared to the Ti@Al substitution, Ti@Na induces a large structural reordering, as observed on the (110) surface in Fig. 4. The titanium atom contracts deeply into the surface and pulls in the surrounding atoms. The Ti atom coordinates to 6 nearest neighbor hydrogen atoms at distances of 1.84–2.00 Å and five Al atoms at 2.61–3.40 Å (average of 3.07 Å); a similar contraction is seen in calculations on bulk substitution of Ti.¹⁴ The equivalent Na-atom in conventional {110} surfaces has five neighboring H atoms at distances of 2.25–2.48 Å and five Al atoms at 3.53–3.79 Å (average of 3.61 Å). In addition to the contraction, the top most (AlH₄)-Na bond is also broken (see Fig. 4).

5.3. Sodium vacancies and NaCl formation

In order for the substitutional process listed above to be thermodynamically feasible, the released Na must form a more stable compound like NaCl. This would require the use of a TiCl_x salt, *e.g.* TiCl₃, and hence a number of additional Na-vacancies must also be created. The energy cost of creating bulk Na-vacancies is found to be as high as 3.7 eV (Table 3) and the surface vacancy formation energies have so far only been investigated in the proximity of titanium on (100) and (001).⁴⁷ The formation energy of surface Na-vacancies is found to depend on the surface structure (see Table 3), and it is energetically preferable to create Na-vacancies on the {110} and {101} type surfaces at a cost of ~3.3 eV. This cost, however, is dramatically reduced when the vacancy is created in the proximity of a surface substituted titanium atom. NaCl formation is consistently observed experimentally when TiCl₃ is used as a dopant for NaAlH₄.

To analyze effects on the decomposition of NaAlH₄ following atomic substitution processes, it is necessary first to analyze the energetics of the formation of sodium surface vacancies and NaCl, respectively. Na-vacancy formation is investigated in the proximity of Ti@Na sites on the closed packed {001} and the more open {110} surfaces. In the case of Ti@Na substituted surfaces with Na-vacancies, a short thermal annealing procedure is performed ($T = 300$ K) using *ab initio* MD simulations, as described in ref. 48. The thermal annealing results in a lower total energy as compared to a direct minimization, which is primarily due to an increased

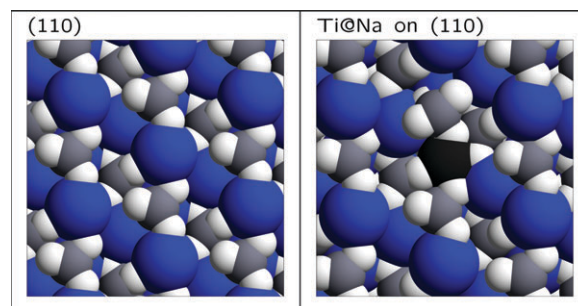


Fig. 4 Substitution of Ti@Na on a (110) surface. Ti (black) is seen to contract into the surface and induce a substantial local re-ordering. For the relative energies, see Table 2.

Table 3 Na-vacancy formation energies with respect to bulk Na

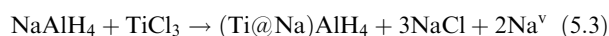
	{001}	—	{110}	—	{101}	{112}	Bulk ^a
Na ^v	3.6	—	3.3	—	3.3	3.5	3.7
Na ^v _{Ti@Na}	1.0 ^b	1.2 ^c	0.8 ^b	0.4 ^c	—	—	—

^a Calculated on a 95 atom super cell, in accordance with ref. 14. ^b Cost of a single vacancy near Ti@Na. ^c Cost of the 2nd vacancy near Ti@Na.

number of Ti–H bonds and rotations of the neighboring AlH₄-complexes.

After cooling, the energy cost is seen to drop to ≤ 1.0 eV for the formation of the first Na-vacancy on the {001} and {110} surfaces, and it is found to be as low as 0.4 eV for a 2nd Na-vacancy on {110}, see Table 3.

It is well documented that TiCl₃ and TiCl₄ are among the best known catalytic additives for cyclic NaAlH₄ hydrogenation,⁴⁹ yet the reason has remained elusive. Based on the obtained results the following pathway for the initial doping process is investigated:



where Na^v is a sodium vacancy. DFT calculations of the ground state energy of NaCl ($E_{\text{form}} = -3.65$ eV) and TiCl₃ ($E_{\text{form}} = -6.35$ eV), respectively, yield the reaction in eqn (5.3) to be favored by 0.6 eV on the {001} surfaces and 1.4 eV on {110} for Ti@NaAlH₄ + 2Na^v. These findings are substantiated by the consistent observation of NaCl in diffraction patterns in TiCl₃ doped samples.⁵⁰ The NaCl is rendered catalytically useless following the initial Ti-deposition process, and henceforth merely reduces the storage capacity, *i.e.* the effect is thus to render atomically dispersed titanium in the matrix. The process is energetically preferred over deposition of atomic Ti, whereas Ti nano-clusters could be comparable.

On {001} Ti@Na + 2Na^v, the Ti atom now coordinates to 7 nearest neighbor (n.n.) hydrogen atoms at distances of 1.86–1.93 Å, one Al atom at 2.77 Å, and four Al atoms at 3.30–3.49 Å. Up to eight n.n. hydrogen atoms have previously been found on this surface.⁴²

On {110} Ti@Na + 2Na^v, the Ti atom coordinates to 7 n.n. hydrogen atoms at distances of 1.84–1.91 Å and two Al surface atoms at 2.78 and 2.82 Å (and two Al at 3.27 and 3.30 Å). With an observed Ti–Al bond length of 2.80 by Léon *et al.*⁴³ and 2.81 Å in TiAl₃,⁵¹ the Ti–Al distances on {001} and {110} are not distinguishable from those in the experimentally observed Ti_xAl_y type species at the surfaces TiCl₃ doped NaAlH₄,^{3,10} and the theoretically proposed formation TiAl_x species on (001).⁴⁷ This is particularly true, if only a minority of the Ti-atoms would remain in these types of surface sites during cycling,⁵² where Ti–Al and Ti–Ti bond lengths appear to fit the gradual development of Ti_{~0.15}Al_{~0.85} type alloys over cycling.^{43,53}

Based on the simulations it is therefore thermodynamically plausible that the Ti atoms or nano-clusters—possibly in the form of Ti(AlH₄)_x type complexes, as *e.g.* suggested by Liu and Ge⁵⁴—can act as catalytic sites for H₂ recombination and/or dissociation.⁵⁵ In the following, the extent of this effect is

quantified by using NEB calculations to determine the potential catalytic effect on the barriers for H₂ desorption.

6. Hydrogen desorption from {001} and {110} surfaces

A key process in the decomposition of NaAlH₄ (eqn (1.1)) is the desorption of molecular hydrogen, which may occur in a number of different ways; the most probable being (i) desorption of H₂ by extraction of hydrogen atoms from two neighboring surface (AlH₄)⁻¹-complexes, and (ii) diffusion of atomic hydrogen from the bulk which recombines at the surface and desorbs as molecular hydrogen.

Hydrogen diffusion in NaAlH₄ is found experimentally to be slow,^{56–58} and although it was recently shown using DFT calculation that bulk substituted Ti lowers the barrier for hydrogen migration¹⁴ in the presence of hydrogen vacancies, the vacancy formation energy is still very high, up to ~ 1.9 eV.⁵⁹ Isotope-scrambling experiments by Bellosta von Colbe *et al.* showed a clear hydrogen–deuterium exchange in the surface region for titanium doped NaAlH₄ which had not been ball-milled, whereas samples ball-milled with TiCl₃ also display bulk hydrogen exchange.⁵ Process (i) is therefore investigated here, analyzing the desorption barriers for both doped and undoped systems.

6.1. Hydrogen desorption from NaAlH₄

The barrier for hydrogen desorption from NaAlH₄ is found to depend on the surface coordination and titanium doping. Desorption barriers have been calculated using NEB (for details on the procedure, see ref. 60) on both the doped and undoped closed packed (001) and the more open (110) surface.

In the calculations on NaAlH₄(001), two surface hydrogen atoms initially separated by 3.23 Å and bound to neighboring (AlH₄)⁻¹-complexes unite and desorb as H₂ following the reaction pathway illustrated in the top row of Fig. 5, with an activation energy as high as 3.0 eV (see Fig. 6). A similar reaction pathway was found on the (110) surface, where the two hydrogen atoms are initially separated by 2.86 Å. The barrier is found to be significantly lower than on (001), although still 2.1 eV. With barriers of this magnitude, it is apparent that catalyst of some sort is needed, if either of these processes are to become the preferred desorption pathways for hydrogen.

6.2. Titanium catalyzed hydrogen desorption

The NaTi@AlH₄ substituted (001) surface and the thermodynamically preferred configurations, where the addition of TiCl₃ induces a Ti substitution for Na on the {001} and {110} surfaces, while creating two neighboring Na-vacancies and three NaCl, are also investigated. Looking first at the desorption pathway on Ti@NaAlH₄(001) + 2Na^v in the second row of Fig. 5, clear differences are seen when compared to the uncatalyzed reaction in the top row. In both cases, the AlH₃-type complexes are seen to shift position in order to compensate for the loss of hydrogen, but on Ti@NaAlH₄(001) + 2Na^v, the presence of Ti induces a large structural reordering of all neighboring AlH_x-complexes, which also lowers the final state energy substantially (see Fig. 6). In fact, the final

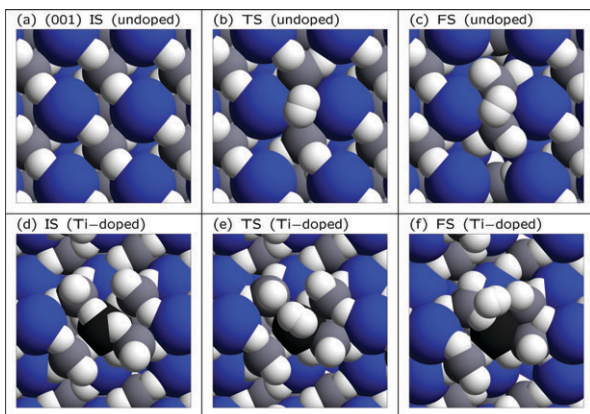


Fig. 5 The H_2 desorption pathway from undoped (a)–(c) and Ti-doped (d)–(f) $\text{NaAlH}_4(001)$ with 2Na^\vee , respectively. (a) & (d) are the initial configurations (IS), (b) & (e) are the transition states (TS), and (c) & (f) are the final states; the corresponding energies can be found in Fig. 6. The neighboring AlH_3 -complexes are seen to move closer in both situations, but the titanium atom (black) induces a large re-ordering and rotation of all neighboring complexes to compensate for the missing hydrogen atoms.

state energy is now slightly below that of the initial state, which is far from the case of the undoped systems, where the final state energy is 1.5 eV higher on (001) and 0.7 eV on (110). A similar effect is observed on the $\text{NaTi@AlH}_4(001)$, where the final and initial state energies are equal.

This lowering of the final state energy can also be viewed as a way of “bypassing” the high hydrogen vacancy formation energy in bulk NaAlH_4 . The created hydrogen “vacancies” can then assist in the release of additional hydrogen by migrating into the particle/crystal. Although the bulk hydrogen vacancy formation energy is very high, the simultaneous creation of Na-vacancies in the presence of Ti@Na -sites was recently shown by Araújo *et al.* to lower this value dramatically.⁸

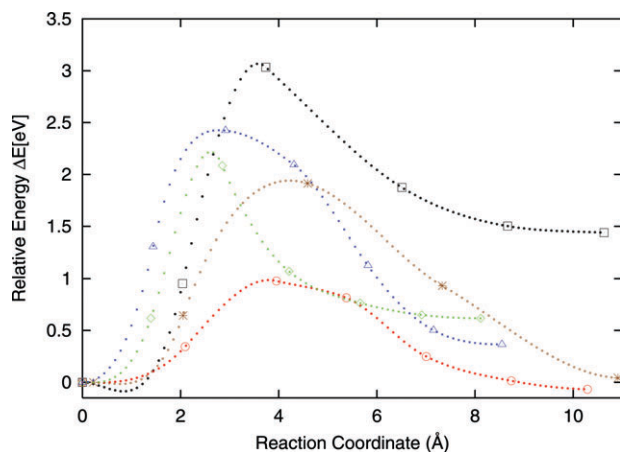


Fig. 6 The calculated barriers for H_2 desorption from $\text{NaAlH}_4(001)$ (□) and a $\text{Ti@NaAlH}_4(001) + 2\text{Na}^\vee$ (○), $\text{NaTi@AlH}_4(001)$ (✱), and H_2 desorption from $\text{NaAlH}_4(110)$ (◇) and $\text{Ti@NaAlH}_4(110) + 2\text{Na}^\vee$ (Δ), respectively. The barrier is seen to be reduced from 3.0 to 1.0 eV for the Ti-catalyzed reaction on {001} surfaces, whereas it remains virtually unchanged on {110} surfaces.

Even more pronounced is the reduction in the barrier for hydrogen desorption on $\text{Ti@NaAlH}_4(001) + 2\text{Na}^\vee$, which is reduced to 0.98 eV; the reduction on $\text{NaTi@AlH}_4(001)$ was found to be smaller, yielding a barrier of 1.9 eV, see Fig. 6. The 0.98 eV is in good agreement with recent experimental work by Luo and Gross, who find an activation energy for the decomposition of Ti-doped NaAlH_4 to Na_3AlH_6 of $86\text{ kJ mol}^{-1}\text{ H}_2$ (0.89 eV).⁶¹ The barrier for the undoped reaction on {001} surfaces is substantially higher than the experimental decomposition energy, but as seen for the {110} surfaces, other facets may have lower barriers, and other desorption pathways may also exist. The pronounced reduction in the barrier height and final state energy on $\text{Ti@NaAlH}_4(001) + 2\text{Na}^\vee$ is in contrast to the negligible effect observed on $\text{Ti@NaAlH}_4(110) + 2\text{Na}^\vee$ (see Fig. 6).

These findings also agree well with the work of Araújo *et al.*,⁵⁹ who find the Ti@Na substitutions weaken the covalent Al–H bond, and thus potentially facilitate the desorption of hydrogen. The presence of Ti is thus seen to lower the barrier substantially on Ti@Na and Ti@Al substituted {001} surfaces, and the catalyzed process appears a likely desorption pathway for hydrogen.

The addition of $\text{Ti}_{13} \cdot 6\text{THF}$ clusters has also been shown to be catalytically effective,³⁴ and deposited Ti nano-cluster can therefore be also expected to be catalytically active. In these situations, the formation of NaCl is no longer a driving force, and titanium can therefore potentially also have other active states. Similarly, any Ti_xAl_y species formed during repeated cycling may also have a kinetic effect.

In the following, the chemical state of titanium in the various configurations on (001) and (110) is analyzed using Wannier functions to determine the chemical state of Ti and to compare it to experimental results.

7. The chemical state of titanium

The charge on the titanium atom depends strongly on the local atomic configuration, *i.e.* the surface structure and the number of neighboring atoms/vacancies. Using localized Wannier functions²⁵ it is possible to calculate the charge on the atom, a value which can be compared directly to EXAFS results obtained under experimental conditions.^{24,28} The value can thus be used as a tool to analyze the correlation between charge and the local atomic configuration.

7.1. Charge distribution in NaAlH_4

Using Wannier functions, the bonding nature of NaAlH_4 is analyzed and it is apparent that ionic bonds are formed between the covalently bonded AlH_4 -complexes and the Na-atoms. In the aluminum complexes, the centers of the four broad s-type orbitals are located at the hydrogen atoms, and the electronic density of states (DOS) is located below the Fermi energy (−8–3 eV), resulting in covalently bonded $(\text{AlH}_4)^{-1.0}$ complexes. The DOS of the s-type Na-orbital is quite narrow (FWHM = 0.166 eV) and located clearly above the Fermi level (1.7 eV), rendering the sodium atoms in the $\text{Na}^{+1.0}$ state.

These findings are in good agreement with literature^{62,63} and provide a sound basis for using Wannier functions to pursue

Table 4 The charges on titanium as determined by integration of the (5d) and (1s) Wannier orbitals, yielding the total charge (ch.)

	(001)				(110)			
	Ti	Na	3Na	Al	Ti	Na	3Na	Al
5d	2.23	1.01	0.47	0.49	1.79	0.48	0.62	0.28
1s	0.05	0.79	0.03	1.69	0.33	0.94	0.0	1.79
ch.	-0.5	+0.4	+3.0	-0.4	-0.2	+1.2	+2.8	-0.1

information about the chemical state of titanium in the various possible surface environments.

7.2. The chemical state of titanium

Five d-like and one s-like Wannier orbitals are initially placed on the titanium atoms; the relaxed shape and occupation depends on the local atomic configuration. By integrating the density of states of the Wannier orbitals localized near the Ti atom up to the Fermi energy, the Ti-charge in the most probable configurations on {001} and {110} surfaces is determined: deposited Ti, Ti@Na, Ti@Na + 2Na^v and Ti@Al. The charge (see Table 4) is seen to depend explicitly on whether Ti has simply been deposited, directly substituted or substituted with Na-vacancy formation. The facets on the other hand are seen to be of little significance.

For Ti deposited on {001} and {110} surfaces, the atom effectively drains charge from the neighboring AlH₄ complexes, forming (AlH₄)^{-0.9} complexes. The titanium atom obtains a weak net negative charge of ~ -0.3 . This charge depletion is likely to induce a destabilization of the neighboring AlH₄ complexes and thus also for NaAlH₄ as a hole, which may induce the transformation into Na₃AlH₆. These findings are in line with the speculations recently proposed by Majzoub *et al.* of Ti-induced AlH₄-destabilization⁶⁴ and also Fichtner *et al.*, who find Ti to influence the nucleation and growth processes.⁶⁵

The obtained charges on Ti@NaAlH₄ + 2Na^v on both (001) and (110) of $\cong +3.0$ do not agree with experimental EXAFS and XANES^{24,28} data on TiCl₃ doped NaAlH₄, where Ti-charges near zero are observed. The reason for this discrepancy could be due to titanium having either multiple species, where a minority species is rate-controlling as stated by Kuba *et al.*³⁹ and also frequently observed in heterogeneous catalysis,^{40,41} or titanium does not only make single atoms substitutions, but forms small nano-sized clusters instead. Recent SEM and TEM analysis have revealed that such Ti-particles must be less than 0.8 nm.⁶⁶

The charge on Ti@Al-sites is, however, found to be close to that of deposited Ti, and hence in good agreement with the EXAFS and XANES experiments, but the Ti@NaAlH₄ + 2Na^v is thermodynamically preferred and the observed barrier reduction on Ti@AlH₄ is less pronounced. Similar charges are expected for Ti nano-clusters and Ti_xAl_y species.

8. Summary

The calculated surface energies of NaAlH₄ result in an equilibrium particle shape which includes {001}, {110}, {101}, and {112} surfaces, but no {100} type surfaces. The complex and multi-facet shapes yield many potential sites for the

ad-/absorption of catalysts, and here, the thermodynamics of Ti deposition and Ti-substitution in the surface layer with/without the simultaneous formation of Na-vacancies is determined. Ti@Al substitution on {110} type facets is found to have the lowest energy cost, although still in excess of 1.1 eV compared to bulk Ti. Direct Ti@Al substitutions are clearly interesting, but the addition of atomic Ti is only thermodynamically viable, if the formation of NaCl is also included, *e.g.* as induced by the preferred catalyst, TiCl₃. In this case, Ti@NaAlH₄ + 2Na^v is stable on both {110} and {001} surfaces. Using NEB calculations, a barrier for H₂ desorption from Ti@NaAlH₄(001) + 2Na^v of slightly below 1.0 eV is obtained, whereas the barrier for NaTi@AlH₄(001) is 1.9 eV and 3.0 eV for undoped desorption. The barrier for the catalyzed desorption on {001} surfaces is in good agreement with the experimentally observed activation energy for dehydrogenation. No effect from the Ti is observed on {110} surfaces, making Ti@NaAlH₄{001} + 2Na^v the preferred pathway for hydrogen desorption and rendering a potential explanation for the pronounced initial catalytic effect of TiCl₃. This effect could persist during the cyclic formation of Ti_xAl_y type species, since only a minority of the titanium would have to be in this surface state.⁵²

The destabilization of NaAlH₄ by Ti-induced charge depletion from neighboring AlH₄-complexes and the subsequent lowering of the barrier for hydrogen desorption and the final state energy, provides a viable explanation for the catalytic role of Ti on the decomposition of NaAlH₄. Although it cannot be concluded whether the proposed catalytic mechanism for enhanced hydrogen desorption is rate-controlling for the decomposition process of NaAlH₄, it agrees well with the observed NaAlH₄ decomposition energy.⁶¹ It is likely that the catalyzed hydrogen desorption is not the only effect of titanium based dopant as found in hydrogen-isotope scrambling experiments,⁵ and further investigations should be undertaken.

Acknowledgements

The author would like to acknowledge the Danish Center for Scientific Computing (DCSC) for supercomputer access and Dr Anders Andreasen and Johannes Voss for valuable comments. The project has received support through the Danish Research Council for Strategic Research (NABIIT).

References

- 1 B. Bogdanović and M. Schwickardi, *J. Alloys Compd.*, 1997, **253–254**, 1.
- 2 L. Schlapbach and A. Züttel, *Nature*, 2001, **414**, 353.
- 3 E. H. Majzoub, J. L. Herberg, R. Stumpf, S. Spangler and R. S. Maxwell, *J. Alloys Compd.*, 2005, **394**, 265.
- 4 F. Schüth, B. Bogdanović and M. Felderhoff, *Chem. Commun.*, 2004, 2249.
- 5 J. M. Bellosta von Colbe, W. Schmidt, M. Felderhoff, B. Bogdanović and F. Schüth, *Angew. Chem., Int. Ed.*, 2006, **45**, 3663.
- 6 S. Chaudhuri and J. T. Muckerman, *J. Phys. Chem. B*, 2005, **109**, 6952.
- 7 D. Sun, T. Kiyobayashi, H. T. Takeshita, N. Kuriyama and C. M. Jensen, *J. Alloys Compd.*, 2002, **337**, L8–L11.
- 8 C. M. Araujo, S. Li, R. Ahuja and P. Jena, *Phys. Rev. B*, 2005, **72**, 165101.
- 9 O. Palumbo, R. Cantelli, A. Paolone, S. S. Srinivasan and C. M. Jensen, *J. Phys. Chem. B*, 2005, **109**, 1168.

- 10 J. Graetz, J. J. Reilly, J. Johnson, A. Y. Ignatov and T. Y. Tyson, *Appl. Phys. Lett.*, 2004, **85**, 500.
- 11 C. Weidenthaler, A. Pommerin, M. Felderhoff, B. Bogdanovic and F. Schüth, *Phys. Chem. Chem. Phys.*, 2003, **5**, 5149.
- 12 O. M. Løvvik and S. M. Opalka, *Phys. Rev. B*, 2005, **71**, 054103.
- 13 O. M. Løvvik and S. M. Opalka, *Appl. Phys. Lett.*, 2006, **88**, 161917.
- 14 J. Voss, Q. Shi, H. S. Jacobsen, M. Zamponi, K. Lefmann and T. Vegge, *J. Phys. Chem. B*, submitted.
- 15 K. Wulff, *Z. Kristallogr. Mineral.*, 1901, **34**, 449.
- 16 B. Hammer and O. H. Nielsen, in *Workshop on Applied Parallel Computing in Physics Chemistry, Engineering Science (PARA95)*, ed. J. Wasniewski, Springer Lecture Notes in Computer Science, Springer, Berlin, 1995, vol. 1041.
- 17 Dacapo pseudopotential code. URL <http://www.fysik.dtu.dk/campos>.
- 18 D. Vanderbilt, *Phys. Rev. B*, 1990, **41**, 7892.
- 19 B. Hammer, L. B. Hansen and J. K. Nørskov, *Phys. Rev. B*, 1999, **59**, 7413.
- 20 H. J. Monkhorst and J. D. Pack, *Phys. Rev. B*, 1976, **13**, 5188.
- 21 G. Kresse and J. Furthmüller, *Comput. Mater. Sci.*, 1996, **6**, 15.
- 22 (a) G. Mills, H. Jónsson and G. Schenter, *Surf. Sci.*, 1995, **324**, 305; (b) H. Jónsson, G. Mills and K. W. Jacobsen, in *Classical and Quantum Dynamics in Condensed Phase Simulations*, ed. B. J. Berne, G. Ciccotti and D. F. Coker, World Scientific, Hackensack, NJ, 1998.
- 23 (a) G. Henkelman and H. Jónsson, *J. Chem. Phys.*, 2000, **113**, 9978; (b) G. Henkelman, B. P. Uberuaga and H. Jónsson, *J. Chem. Phys.*, 2000, **113**, 9901.
- 24 A. Léon, O. Kircher, J. Rothe and M. Fichtner, *J. Phys. Chem. B*, 2004, **108**, 16372.
- 25 G. H. Wannier, *Phys. Rev.*, 1937, **52**, 191.
- 26 K. S. Thygesen, L. B. Hansen and K. W. Jacobsen, *Phys. Rev. Lett.*, 2005, **94**, 026405.
- 27 K. S. Thygesen and K. W. Jacobsen, *Phys. Rev. Lett.*, 2005, **94**, 036807.
- 28 M. Felderhoff, K. Klementiev, W. Grünert, B. Splithoff, B. Tesche, J. M. Bellosta von Colbe, B. Bogdanović, M. Härtel, A. Pommerin, F. Schüth and C. Weidenthaler, *Phys. Chem. Chem. Phys.*, 2004, **6**, 4369.
- 29 L. P. Van, J. Cousty and C. Lubin, *Surf. Sci.*, 2004, **549**, 157.
- 30 T. J. Frankcombe and O. M. Løvvik, *J. Phys. Chem. B*, 2006, **110**, 622.
- 31 V. Fiorentini and M. Methfessel, *J. Phys.: Condens. Matter*, 1996, **8**, 6525.
- 32 J. Chen, N. Kuriyama, Q. Xu, H. T. Takeshita and T. Sakai, *J. Phys. Chem. B*, 2001, **105**, 11214.
- 33 A. Andreasen, T. Vegge and A. S. Pedersen, *J. Solid State Chem.*, 2005, **178**, 3672.
- 34 M. Fichtner, O. Fuhr, O. Kircher and J. Rothe, *Nanotechnology*, 2003, **14**, 778.
- 35 H. W. Brinks, M. Sulic, C. M. Jensen and B. C. Hauback, *J. Phys. Chem. B*, 2006, **110**, 2740.
- 36 V. P. Balema and L. Balema, *Phys. Chem. Chem. Phys.*, 2005, **7**, 1310.
- 37 E. H. Majzoub and K. J. Gross, *J. Alloys Compd.*, 2003, **356–357**, 363.
- 38 P. Wang, X. D. Kang and H. M. Cheng, *J. Phys. Chem. B*, 2005, **109**, 20131.
- 39 M. T. Kuba, S. S. Eaton, A. Morales and C. M. Jensen, *J. Mater. Res.*, 2005, **20**, 3265.
- 40 K. Honkola, A. Hellman, I. N. Remediakis, A. Logadottir, A. Carlsson, S. Dahl, C. H. Christensen and J. K. Nørskov, *Science*, 2005, **307**, 555.
- 41 R. T. Vang, K. Honkala, S. Dahl, E. K. Vestergaard, J. Schnadt, E. Laegsgaard, B. S. Clausen, J. K. Nørskov and F. Besenbacher, *Nat. Mat.*, 2005, **4**, 160.
- 42 J. Íñiguez, T. Yildirim, J. Udovic, M. Sulic and C. M. Jensen, *Phys. Rev. B*, 2004, **70**, 060101.
- 43 A. Léon, O. Kircher, M. Fichtner, J. Rothe and D. Schild, *J. Phys. Chem. B*, 2006, **110**, 1192.
- 44 T. Vegge *et al.*, unpublished work.
- 45 J. L. Herberg, R. S. Maxwell and E. H. Majzoub, *J. Alloys Compd.*, 2006, **417**, 39.
- 46 M. Fichtner, Transformation Mechanisms of Alanate Composites, *IPHE International Hydrogen Storage Conference*, Lucca, Italy, 2005, <http://www.iphe.net/StorageLuccaposters.htm>.
- 47 T. Yildirim and Íñiguez, *Appl. Phys. Lett.*, 2005, **86**, 103109.
- 48 Z. Lodziana and T. Vegge, *Phys. Rev. Lett.*, 2004, **93**, 145501.
- 49 D. L. Anton, *J. Alloys Compd.*, 2003, **356**, 400.
- 50 A. Léon, D. Schild and M. Fichtner, *J. Alloys Compd.*, 2005, **404**, 766.
- 51 C. Colinet and A. Pasturel, *J. Phys.: Condens. Matter*, 2002, **14**, 6713.
- 52 A. Léon, O. Kircher, M. Fichtner, J. Rothe and D. Schild, *J. Phys. Chem. B*, 2006, **110**, 1192.
- 53 H. W. Brinks, B. C. Hauback, S. S. Srinivasan and C. M. Jensen, *J. Phys. Chem. B*, 2005, **109**, 15780.
- 54 J. J. Liu and Q. F. Ge, *Chem. Commun.*, 2006, **17**, 1822.
- 55 T. Vegge, A. Andreasen and A. S. Pedersen, in *Technologies for sustainable energy development in the long term. Proceedings of Risø International Energy Conference 2005*, ed. L. S. Petersen and H. Larsen., Risø National Laboratory, Roskilde, Denmark, 2005, pp. 105–115.
- 56 G. Majer, E. Stanik, L. E. Valiente Banuet, F. Grinberg, O. Kircher and M. Fichtner, *J. Alloys Compd.*, 2005, **738**, 404–406.
- 57 A. Andreasen, J. i. Højllum, T. Vegge, D. Engberg, C. Niedermayer and K. Lefmann, *A QENS study of hydrogen motion in NaAlH₄*, in *SINQ - experimental report*, 2005, p. 1, http://sinq-web.psi.ch/sinq/er/ii_04r_10.pdf.
- 58 Q. Shi, H. S. Jacobsen, J. Voss and T. Vegge, unpublished work.
- 59 C. M. Araújo, R. Ahuja, J. M. O. Guillén and P. Jena, *Appl. Phys. Lett.*, 2005, **86**, 251913.
- 60 T. Vegge, *Phys. Rev. B*, 2004, **70**, 034512.
- 61 W. Luo and K. J. Gross, *J. Alloys Compd.*, 2004, **385**, 224.
- 62 A. Aguayo and D. J. Singh, *Phys. Rev. B*, 2004, **69**, 155103.
- 63 A. Peles, J. A. Alford, Z. Ma, Li Yang and M. Y. Chou, *Phys. Rev. B*, 2004, **70**, 165105.
- 64 E. H. Majzoub, K. F. McCarty and Ozolinš, *Phys. Rev. B*, 2005, **71**, 024118.
- 65 M. Fichtner, P. Canton, O. Kircher and A. Léon, *J. Alloys Compd.*, 2005, **404–406**, 732.
- 66 A. Léon, O. Kircher, H. Rösner, B. Décamps, E. Leroy, M. Fichtner and A. Perceron-Guégan, *J. Alloys Compd.*, 2006, **414**, 190.